Effect of Polycarbonate Molecular Weight on Precrack Hysteresis Energy in Determining its Ductile-Brittle Transition

FENG-CHIH CHANG* and HON-CHUN HSU

Institute of Applied Chemistry, National Chaio-Tung University, Hsinchu, Taiwan, Republic of China

SYNOPSIS

The distinctive ductile-brittle transition behavior of pseudoductile polymeric materials such as polycarbonate (PC) has been discovered to be closely related to the precrack hysteresis loss energy. The higher molecular weight (MW) PC with higher ductility also results in higher precrack hysteresis energy and therefore greater precrack plastic volume under condition of constant loads. If the precrack plastic volume exceeds a critical value, crack initiation thereafter will propagate within the domain of the plastic zone and results in ductile fracture. The deformation displacement is closely related to the precrack plastic volume, and the critical displacement actually determines the critical plastic volume. The higher molecular weight polycarbonate with higher entanglement density is able to withstand earlier crack initiation more effectively. Toughening plastics, such as rubber modification, is simply the result of delaying or retarding the crack initiation and allows the precrack plastic zone to grow over its critical value. A model of crack criterion based on precrack plastic zone is proposed to interpret the ductile-brittle transition phenomenon.

INTRODUCTION

Polycarbonate, a pseudoductile polymeric matrix, has a considerably lower shear yield stress and a distinctive ductile-brittle transition in the notch specimens in response to numerous variables such as thickness, orientation, deformation rate, temperature, physical aging, notch radius, molecular weight, and elastomer content. The mechanism of such sharp transition is not fully understood due to its extreme complexity, and the subject has attracted great attention for practical safety reason. Polymeric materials with gradual ductile-brittle transition usually can be properly interpreted with classical or modified fracture mechanics. However, fracture mechanics is not particularly suitable in interpreting the sharp ductile-brittle transition phenomenon. Pitman[1] accounted for the phenomenon such as polycarbonate (PC) in terms of a competition between shear yielding and crazing. Effect of molecular weight and its distribution on mechanical behavior of polymers has been well recognized.[2] Many glassy polymers have very low mechanical strengths; strength increases as the MW is increased, and eventually reaches a constant level at a critical MW. Studies on the effect of polycarbonate MW on tensile fracture stress,[3] tensile impact,[4] notch impact,[5-8] and fracture energy G_c[7,9] have been previously reported. Both the classical LEFM and the J integral concepts assume the potential energy is consumed exclusively for the propagation of the crack and neglect the energy associated with plasticity or viscoelasticity. Part of the precrack inelastic energy eventually converts into a heat and plastic zone ahead of the crack tip. For the brittle materials, fracture mechanics is considered applicable because the plastic zone is small and limited around the crack tip. In cases of ductile fracture, the precrack hysteresis energy and plasticity are too significant to be neglected. The total input energy at onset of the crack initiation is consisted of elastic storage and inelastic plastic energies. The precrack hysteresis (loss) energy should correlate with the size of the plastic zone for those pseudoductile matrices. If the

* To whom correspondence should be addressed.

Journal of Applied Polymer Science, Vol. 43, 1025–1036 (1991)

 CCC 0021-8995/91/061025-12$04.00

Table I Melt Flow Rates of Polycarbonates

Dow Spec. MFR	Original Pellets	Injection Molded
3	3.10	3.35
6	6.89	7.78
10	10.61	12.08
15	14.85	15.47
20	21.75	22.23
60[a]	60.81	63.48
80[a]	—	80.32

Melt flow rates were determined as g/10 min at 300°C using a Melt Flow Indexer from Ray-Ran.

[a] Experimental product from Dow.

size of the precrack plastic zone exceeds a critical value prior to the onset of crack initiation, the crack developed later will propagate through the plastic zone and results in ductile fracture as long as the crack front propagates within the plastic zone. If the precrack plastic zone is too small at the onset of crack initiation to contain the propagating crack front, a brittle or semiductile failure occurs. Our recent studies showed a close relation between precrack hysteresis energy and ductile-brittle transition of notch polycarbonate in terms of molecular weight, elastomer content, temperature, notch radius, strain rate, and annealing.[7,8,10–14] It is interesting to note that essentially all trends observed coincide with the ductile-brittle transition behavior of polycarbonate. Therefore, the most important factor in determining the ductile-brittle transition is probably the precrack hysteresis energy (and thus plastic zone size) or the deformation displacement at crack initiation. Any effort to toughen the pseudoductile matrices delays or retards the crack initiation for allowing the growth of the plastic zone over its critical value. The concept of a critical precrack plastic zone is proposed to interpret the ductile-brittle transition behavior.

EXPERIMENTAL

Nature-grade polycarbonate samples with melt flow rates (MFRs) from 3–80 were kindly donated by Dow Chemical Company, and their molecular weights, densities, impact, and tensile properties were previously reported.[7] Table I shows the experimental MFRs of the injection-molded parts and the original pellets. The results indicate excellent MFR control from the manufacturer. Specimens of dimensions $6 \times \frac{1}{2} \times \frac{1}{8}$ and $6 \times \frac{1}{2} \times \frac{1}{4}$ in were injection molded using a 3-oz Arbury molding machine according to the manufacturer's recommended conditions. Standard notch radius of 10 mils (0.25 mm) was carried out using a single tooth cutter. The device and specimen dimension for the slow rate fracture and hysteresis studies are shown in Figure 1, and the detailed procedures were previously reported.[15] Experiments at ambient conditions and a single constant displacement-controlled rate of 10 mm/min have been maintained throughout this study. The scanning electron microscopy (SEM) of the fractured surface was carried out on a Hitachi S-570 scanning electron microscope after being sputter-coated with Au.

RESULTS AND DISCUSSION

Slow Rate Total Fracture

Polycarbonate specimens with 10-mils notch radius and $\frac{1}{8}$-in thickness were fractured in ductile mode

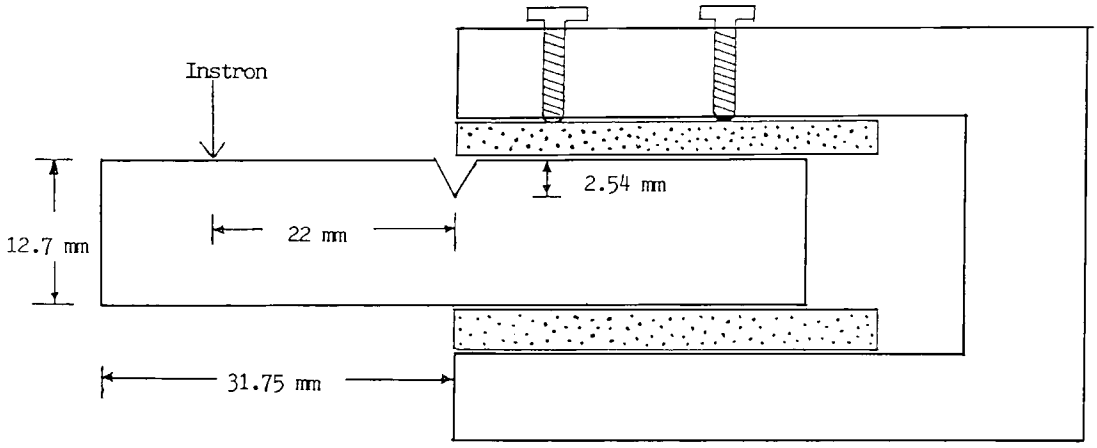

Figure 1 The clamp device for slow-rate deformation-fracture and hysteresis cyclic studies.

Table II Slow Rate Fracture for $\frac{1}{4}$-in. Polycarbonates

Sample MFR, No. Runs	Total Fracture Energy, J	Crack Initiation Energy, J	Crack Initiation Disp., mm	Maximum Load KN	Ductile or Brittle
3, (4)	4.160 ± 0.127	1.358 ± 0.018	4.456 ± 0.026	0.469 ± 0.007	D
6, (4)	4.110 ± 0.118	1.371 ± 0.044	4.492 ± 0.013	0.479 ± 0.017	D
10, (3)	4.081 ± 0.561	1.289 ± 0.184	4.428 ± 0.358	0.450 ± 0.037	D
10, (3)	0.592 ± 0.187	0.588 ± 0.191	2.680 ± 0.410	0.371 ± 0.062	B
15, (5)	0.425 ± 0.071	0.419 ± 0.015	2.146 ± 0.126	0.369 ± 0.038	B
20, (5)	0.400 ± 0.056	0.394 ± 0.057	2.336 ± 0.186	0.336 ± 0.025	B
60, (4)	0.0336 ± 0.0040	0.0165 ± 0.0046	0.623 ± 0.182	0.067 ± 0.020	B

even under impact rate (3 m/sec) at ambient temperature except those from MFR = 60 and 80.[7] For the thicker $\frac{1}{4}$-in specimens, they all fractured in brittle mode under the same IZOD impact conditions except the one with MFR = 3, which was near its ductile-brittle transition.[16] Table II and Figure 2 summarize data of total fracture and load-displacement curves of the typical $\frac{1}{4}$-in PC samples with various MFRs. PCs with MFR = 3 and 6 (curves A and B, Fig. 2) fracture in a typical ductile mode, showing clear propagation energy. PCs with MFR = 15 and 20 (curves E and F, Fig. 2) fracture in brittle mode with only initiation energy and no propagation energy. PC with MFR = 60 shows stable cracking after crack initiation with clear propagation energy, but has very small cracking load, total fracture energy, and crack initiation displacement. Regular PC is known for its unstable crack propagation in a typical fracture mechanics study unless at low temperature (−40°C). PC with MFR = 10 (curves C and D, Fig. 2) exists in either ductile or brittle fracture, an indication of ductile-brittle transition

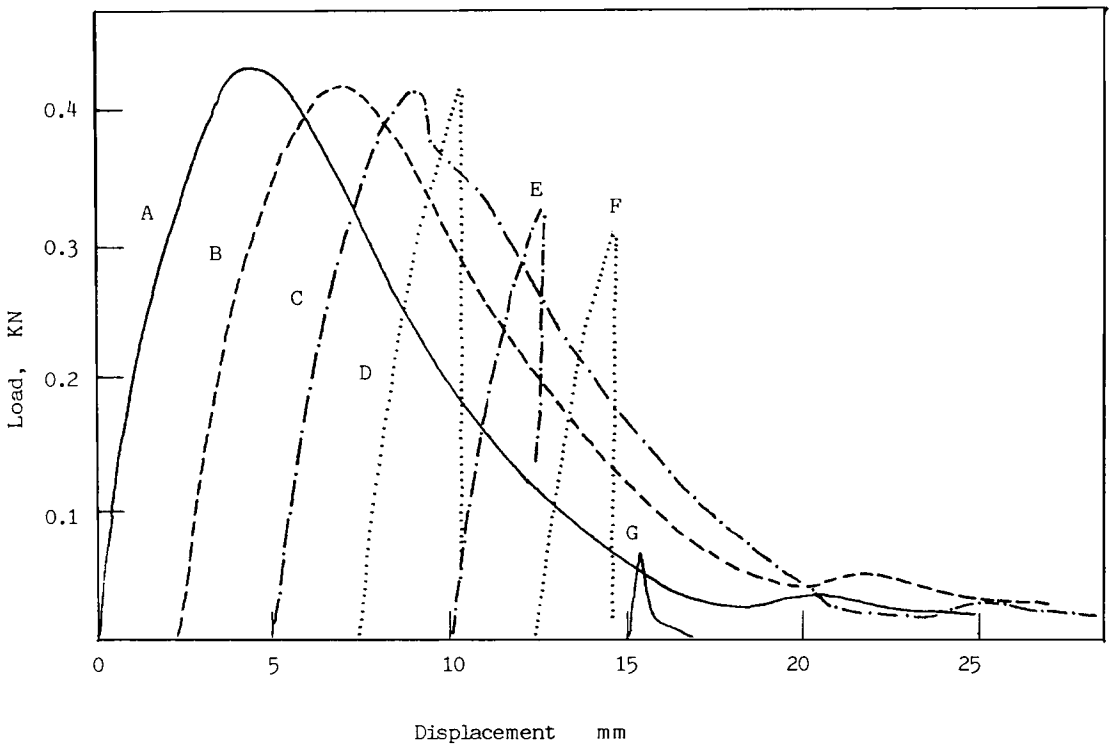

Figure 2 Typical load-displacement curves for polycarbonates, $\frac{1}{4}$ inch thickness, 10 mils notch, 10 mm/min deformation rate, and at ambient temperature. A, MFR = 3, ductile; B, MFR = 6, ductile; C, MFR = 10, ductile; D, MFR = 10, brittle; E, MFR = 15, brittle; F, MFR = 20, brittle; G, MFR = 60, brittle.

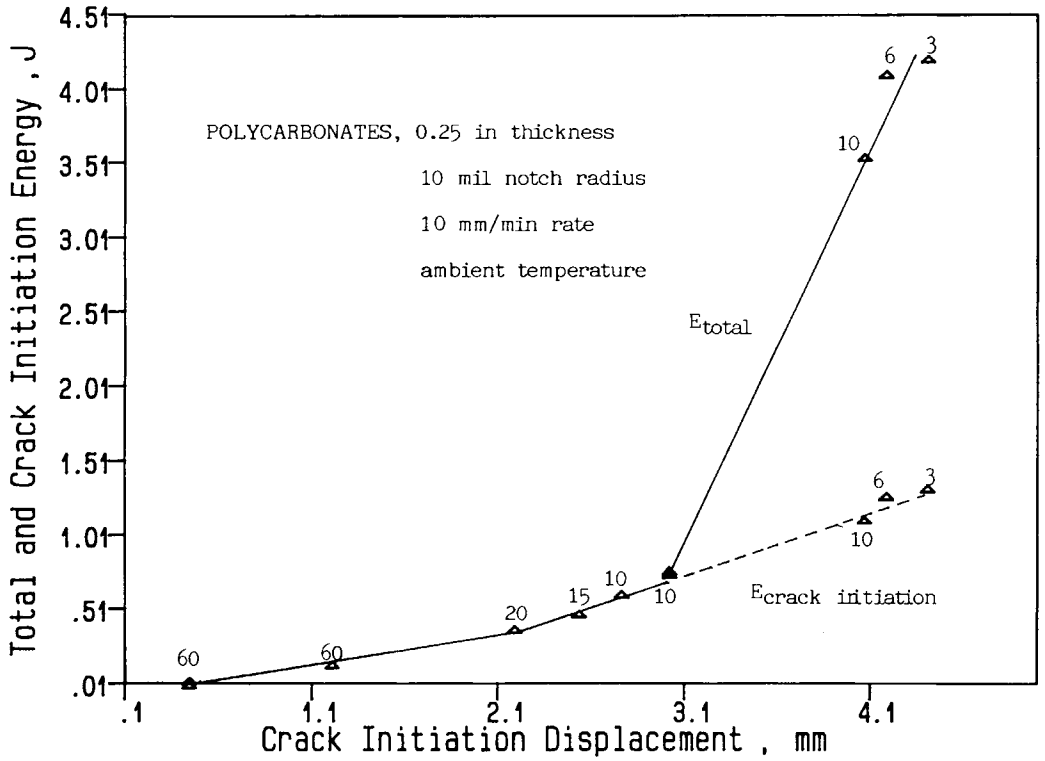

Figure 3 Plots of crack initiation displacement vs. total fracture energy and crack initiation energy for PC with various MFRs. Data come from individual runs, not from Table II average; most data points match Figure 2.

conditions. Detection of crack initiation is difficult for those ductile-fractured specimens and usually occurs just prior to the load maximum.[17] For convenience, load maximum is taken as crack initiation in our discussion. Those brittle fracture specimens, such as MFRs = 15, 20, and 60, are very unstable in terms of cracking load, initiation displacement, and fracture energy, and the curves shown in Figure 2 are samples selected with representative nature. Figure 3 demonstrates that the crack initiation energy is increased with the increase of crack initiation displacement (displacement at load maximum) and PC MFR (admittedly not very consistent, but the trend is there). The crack initiation energy and total fracture energy are very close for those brittle failed PCs except the one with stable cracking (MFR = 60). Figure 3 clearly demonstrates the importance of crack initiation displacement in dictating the behavior of the resultant fracture, ductile or brittle mode. PC with lower MFR (higher MW) has higher entanglement density and lower yield stress,[7] which is able to resist crack initiation more effectively and results in greater crack initiation displacement and thus becomes more ductile. Since part of the input energy prior to the onset of crack initiation is consumed as inelastic, plastic energy and the precrack plastic zone is expected to be increased with the increase of deformation displacement. As soon as the precrack displacement or the plastic zone exceeds a certain critical level, any crack developed thereafter will be effectively contained within the domain of the plastic zone and results in ductile tearing. Figure 3 shows that the critical displacement for the ductile-brittle transition of the $\frac{1}{4}$-in PC is about 3.1 mm. The SEM photomicrographs of the corresponding fractured surfaces are shown in Figures 4(a)-4(f). For the ductile fracture, the surface appears distorted and irregular with clear lateral constriction. The higher MW PC has less striating lines on the surface, indicating better resistance to tearing after extensive yielding, and results in higher fracture energy, very similar to our previous results from the $\frac{1}{8}$-in impact fracture surfaces.[7] For the brittle fractured surfaces, large numbers of brittle type striating lines are present but no lateral constriction can be observed. The MFR = 60 [Fig. 4(f)] has the lowest total fracture energy, showing less striating lines with rather smooth surface between lines.

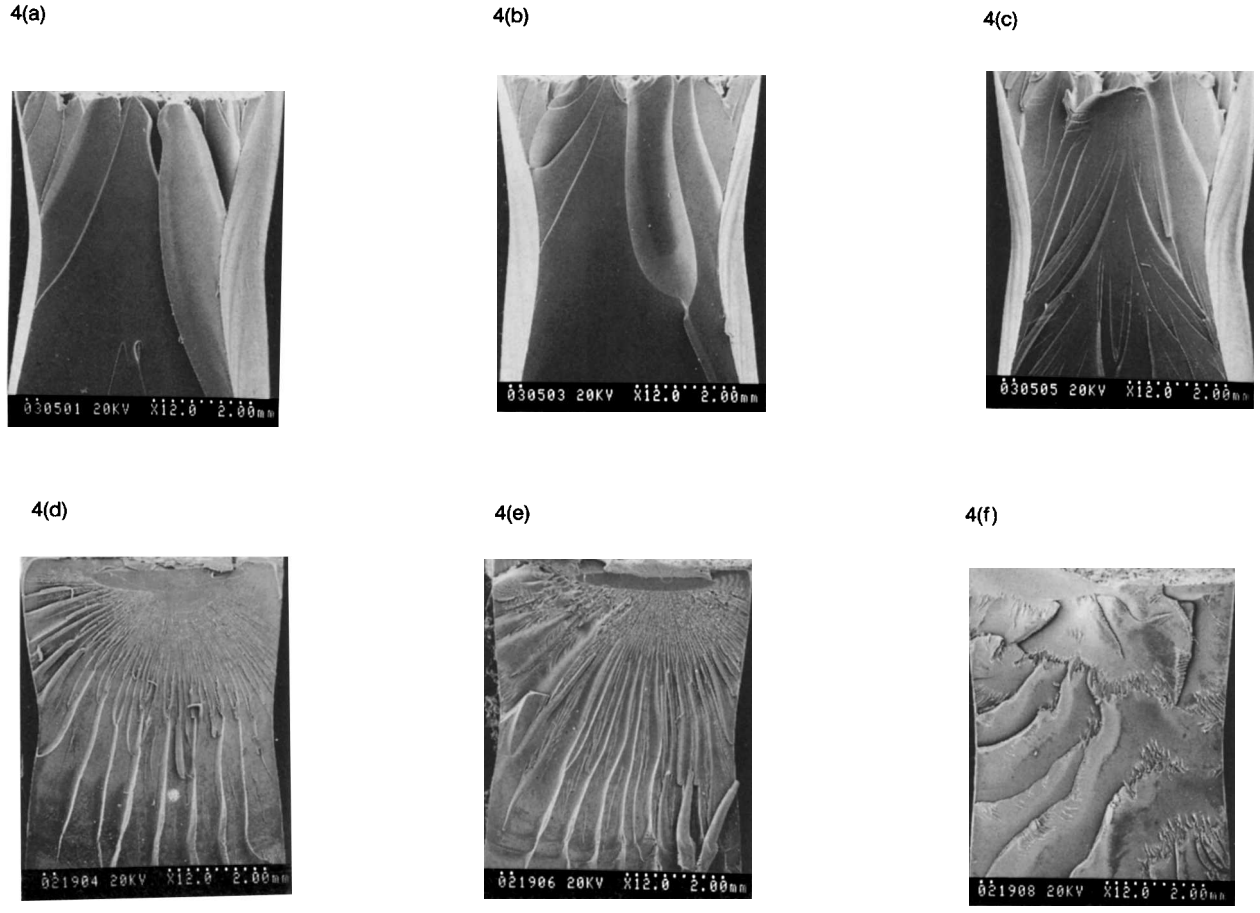

Figure 4 SEM photomicrographs of PC fracture surfaces from Figure 2. a, MFR = 3, ductile, 4.220 J; b, MFR = 6, ductile, 3.990 J; c, MFR = 10, ductile, 3.772 J; d, MFR = 10, brittle, 0.405 J; e, MFR = 20, brittle, 0.373 J; f, MFR = 60, brittle, 0.034 J.

Precrack Hysteresis under Different Loads

Hysteresis, the term can only be applied strictly when the deformed material returns to its original shape (i.e., zero permanent displacement). Most previous work on hysteresis has been carried on tensile specimens. Narisawa and Takemori[18] recently reported the hysteresis loss of the notched ABS and PBT/PC samples and related the input and dissipated energies. The typical example of the cyclic load–unload curves by using the displacement-controlled condition for the $\frac{1}{8}$-in polycarbonate (MFR = 15) is demonstrated in Figure 5. A higher load results in higher displacement, percent hysteresis, and permanent displacement. The precrack hysteresis loop can occur due to viscoelasticity, plasticity, and crazes or microvoids for certain less ductile polymeric materials. These three or four types of energy dissipation processes do not occur separately but are superimposed upon each other. Distinction among them or quantifying these complicated and overlapping processes in any deformation stage is very difficult, if not impossible. However, the trend of higher hysteresis loss resulting in greater precrack plasticity is undeniable. The similar trend has also been observed from permanent displacement, considered the most convincing evidence of precrack plasticity. Slight load bounces at the peaks of the hysteresis loops are indicative of the viscoelastic nature of polymeric materials. As expected, the extent of load bounce is increased with the increase of deformation rate (will report later) and the decrease of load level. At the load of 0.05 KN (curve A, Fig. 5), the unloading line actually stays above the loading line and results in a negative hysteresis. To minimize such load bouncing problems and reduce the importance of viscoelasticity in the hysteresis loss, a fairly slow deformation rate of 10 mm/min has been purposely chosen in this study.

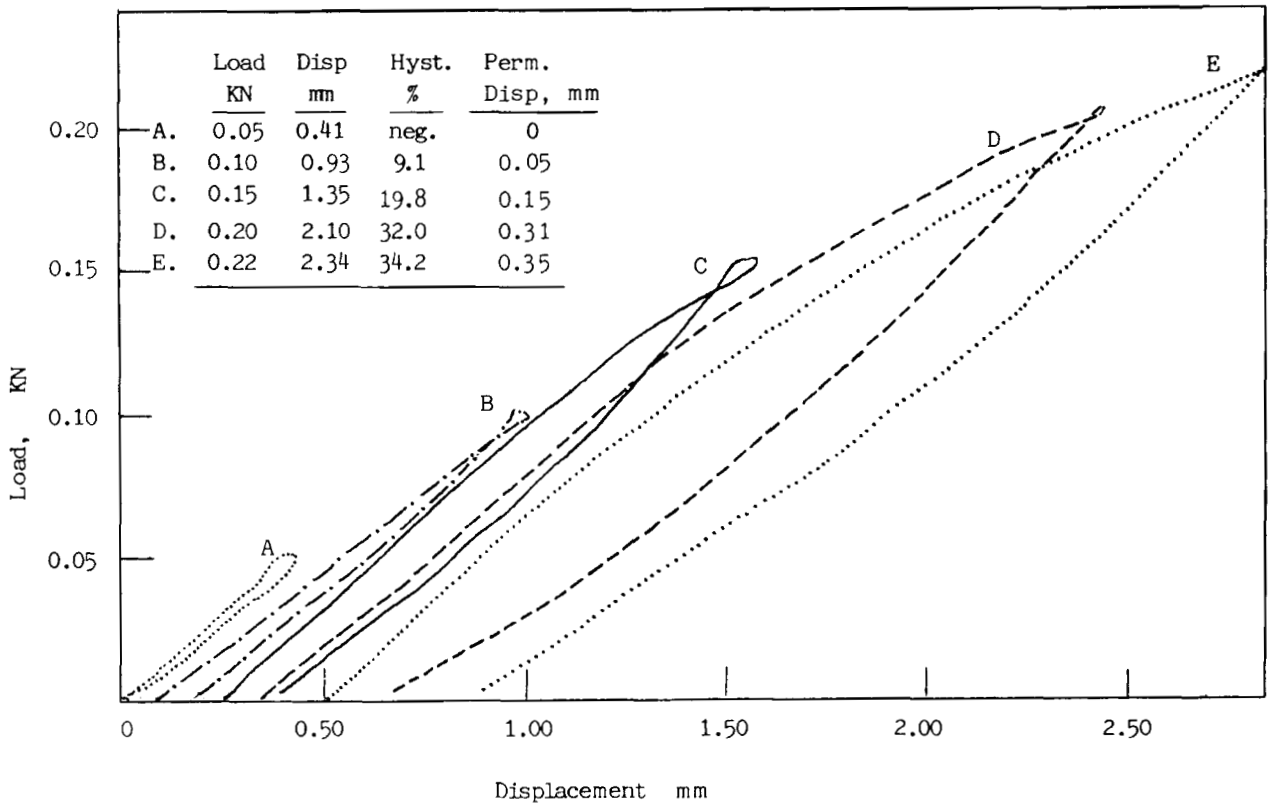

Figure 5 Example of load-displacement curves from the hysteresis cycles at various load levels for $\frac{1}{8}$-in PC, MFR = 15.

Precrack Hysteresis of Various MFR Polycarbonates

Due to polycarbonate's brittle nature for thicker specimens ($\frac{1}{4}$ inch), the maximum obtainable loads are very unstable and rather low except those from the low-MFR PCs. Therefore, PC specimens with $\frac{1}{8}$ inch thickness were chosen to investigate the precrack hysteresis. Data are summarized in Table III and Figures 6–9. Three load levels selected in this study (0.10, 0.15, and 0.20 KN) are believed all prior to the onset of crack initiation. Figure 6 shows the plots of percent hysteresis loss vs. loads for PC with various MFRs. The results demonstrate a clear trend of higher percent hysteresis loss from the lower-MFR specimens at constant loads, even though some data points are scattering. Figure 7 displays the relation of percent hysteresis loss and the corresponding displacement, and again shows the higher MFR resulting in lower displacement and lower percent hysteresis loss at constant loads. Yield stress and modulus from different MFR PCs appear to be important or at least partially responsible for the observed results. Our previous study showed the tensile yield stress and modulus were increased with increase of MFR.[7] Figure 8 shows a similar plot by employing the hysteresis energy instead of the percent hysteresis loss; however, the results seem better fit into a master curve relating precrack hysteresis energy and deformation displacement, but nearly independent of the PC MFR. That means the precrack hysteresis energy is heavily dependent on deformation displacement rather than on PC MFR. Figure 9 illustrates the relation between precrack hysteresis energy and the resultant permanent displacement. As mentioned above, if the hysteresis comes strictly from viscoelasticity, the corresponding permanent displacement should be zero. Greater permanent displacement is indicative of greater precrack plasticity and thus greater precrack plastic zone (crazes or microvoids in this ductile material are negligible). It is obviously clear now that a close relation exists between the precrack hysteresis energy and size of the precrack plastic zone.

Critical Hysteresis Energy and Critical Displacement

As previously mentioned, we are unable to observe the ductile-brittle transition from the $\frac{1}{8}$-in. speci-

Table III Summarized Hysteresis Data for $\frac{1}{8}$-in. Polycarbonates

Sample, MFR	Load, KN 0.20	0.15	0.10
3 Displacement, mm	2.48	1.45	1.09
Permanent Disp., mm	0.590	0.220	0.089
Total Energy, J	0.286	0.118	0.055
% Hysteresis	41.1	26.7	13.4
Hyst., Energy, J	0.118	0.032	0.0074
6 Displacement, mm	2.37	1.41	1.01
Permanent Disp., mm	0.433	0.208	0.077
Total Energy, J	0.282	0.117	0.052
% Hysteresis	37.1	24.7	13.1
Hyst., Energy, J	0.105	0.029	0.0068
10 Displacement, mm	2.29	1.40	0.97
Permanent Disp., mm	0.422	0.172	0.070
Total Energy, J	0.273	0.112	0.049
% Hysteresis	37.0	22.3	12.9
Hyst., Energy, J	0.101	0.025	0.0063
15 Displacement, mm	2.23	1.35	0.93
Permanent Disp., mm	0.327	0.155	0.045
Total Energy, J	0.265	0.115	0.047
% Hysteresis	32.6	19.8	9.1
Hyst., Energy, J	0.086	0.023	0.0043
20 Displacement, mm	2.12	1.15	0.88
Permanent Disp., mm	0.317	0.108	0.037
Total Energy, J	0.244	0.097	0.042
% Hysteresis	32.1	15.4	6.0
Hyst., Energy, J	0.078	0.015	0.0025
60 Displacement, mm	2.08	1.10	0.82
Permanent Disp., mm	0.175	0.095	0.031
Total Energy, J	0.236	0.091	0.040
% Hysteresis	25.2	15.1	5.4
Hyst., Energy, J	0.059	0.014	0.0022

mens under the chosen condition, but have to rely on them to obtain the MFR-related hysteresis information. Figure 8 demonstrates the fairly close relation between hysteresis energy and displacement disregarding the MFR. It is not unreasonable to assume that such a relation can be extended to the thicker ($\frac{1}{4}$-inch) specimens. Therefore, we should be able to construct the similar hysteresis energy vs. displacement curve based on lower MFR PC with load up to near its crack initiation. By comparing this curve with the critical displacement data in Figure 3, the critical hysteresis energy can thus be obtained. Figure 10 shows the constructed curve of the precrack hysteresis energy vs. displacement only from two MFR PCs, where the critical displacement of about 3.1 mm is obtained from Figure 3. The critical hysteresis energy is estimated from the intercept of the critical displacement and the curve of the precrack hysteresis energy vs. displacement. The critical hysteresis energy of about 0.16 J for the $\frac{1}{4}$-in. PC is thus determined. Since the energy dissipation through crazes, microvoids, and viscoelasticity are relatively insignificant under the chosen conditions and the selected materials as previously mentioned, the precrack hysteresis energy is mainly consumed in creating the precrack plastic zone and partially converted into heat. In an attempt to measure the temperature rise at the crack tip by using a crude IR thermometer on an area much larger than desirable, a total rise of 4°C was recorded on the $\frac{1}{8}$-in. sample. How to correlate precrack hysteresis energy and the corresponding precrack plastic volume is important only for physical meaning and will not be discussed in details in this article.

Ductile-Brittle Transition Criterion

The trends of the observed precrack hysteresis coincide with the ductile-brittle transition behavior for polycarbonates. Therefore, it is not unreasonable to correlate between the material precrack hysteresis energy and its ductile-brittle transition behavior. The precrack plastic zone is directly related to the corresponding hysteresis energy although their relation is highly complicated and dependent of testing variables and materials. Even the shape of the precrack plastic zone can be different, especially from different specimen geometries. A preliminary model based on precrack plastic zone is proposed to interpret the ductile-brittle transition phenomenon for the pseudoductile polymeric materials that neglects the shape of plastic zone and the energy dissipations due to crazes or microvoids. The reason we chose the more complicated plastic zone instead of using hysteresis energy directly obtainable is easier understood in terms of physical meaning. The size of a precrack plastic zone is function of deformation rate (v), temperature (T), specimen thickness (B), notch radius (r), deformation displacement (L), yield stress (∂_y), and molecular weight (M).

$$V_p = f(v, T, B, r, L, \partial_y, M). \quad (1)$$

Total input energy consists of elastic storage and inelastic hysteresis energy. The inelastic hysteresis energy can be obtained experimentally from the in-

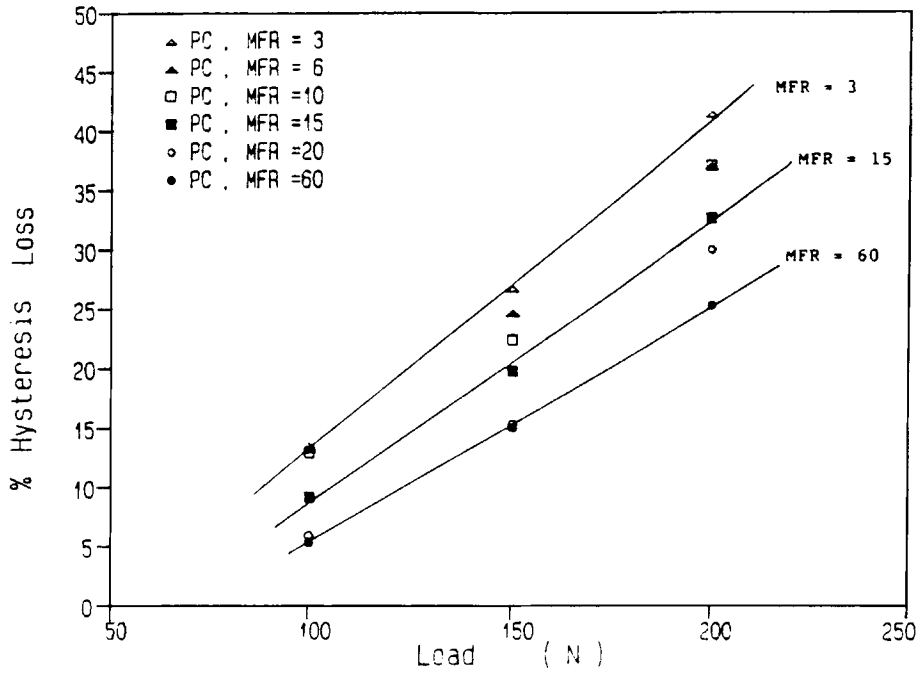

Figure 6 Plots of load vs. percent hysteresis loss for $\frac{1}{8}$-in. PC with various MFRs.

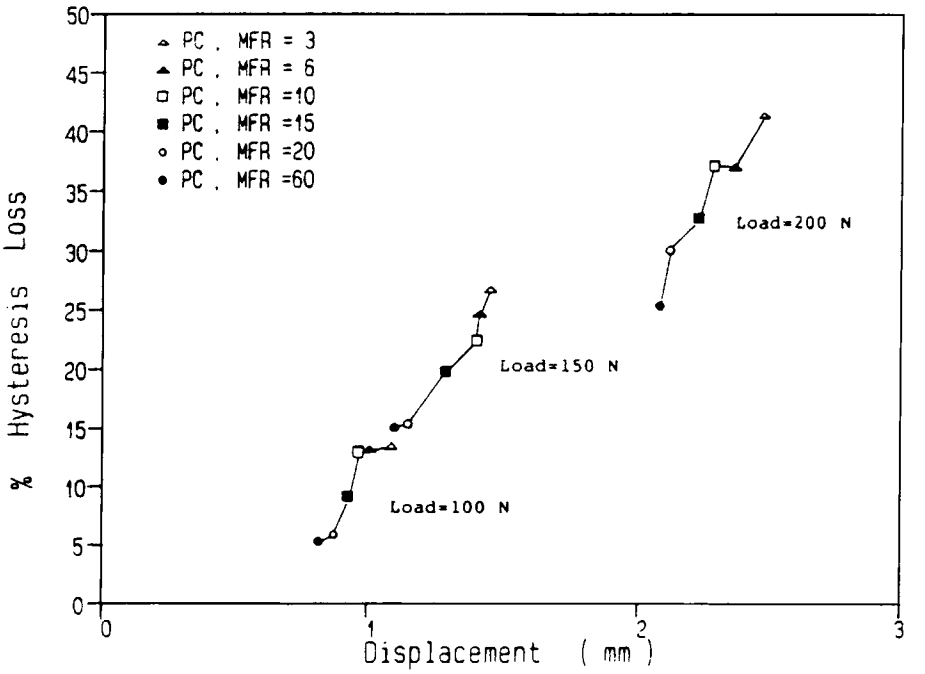

Figure 7 Plots of deformation displacement vs. percent hysteresis loss for PC with various MFRs.

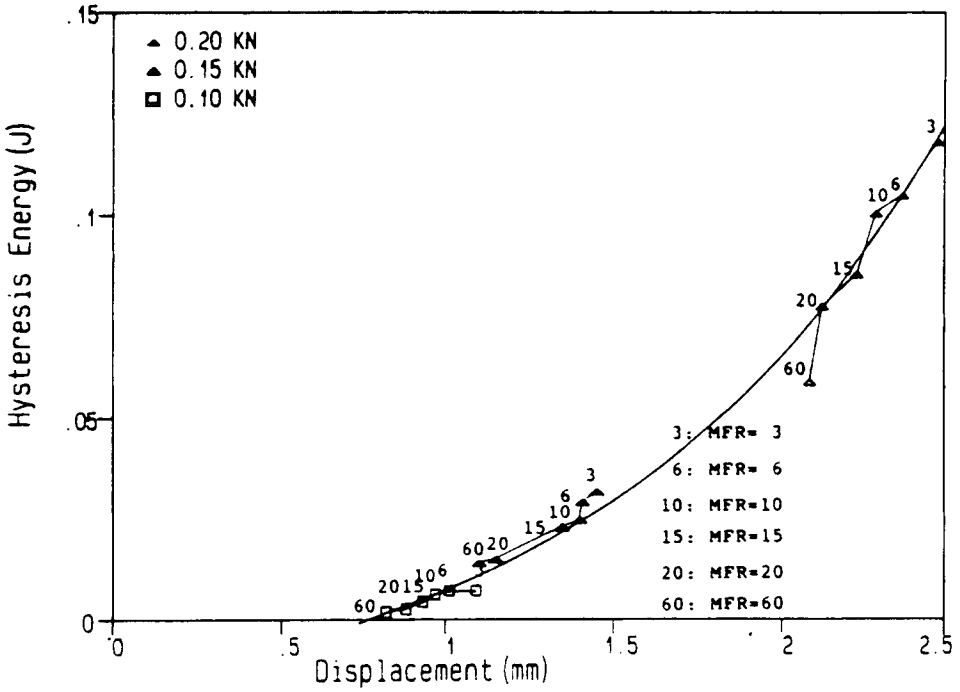

Figure 8 Plots of deformation displacement vs. hysteresis energy for PC with various MFRs.

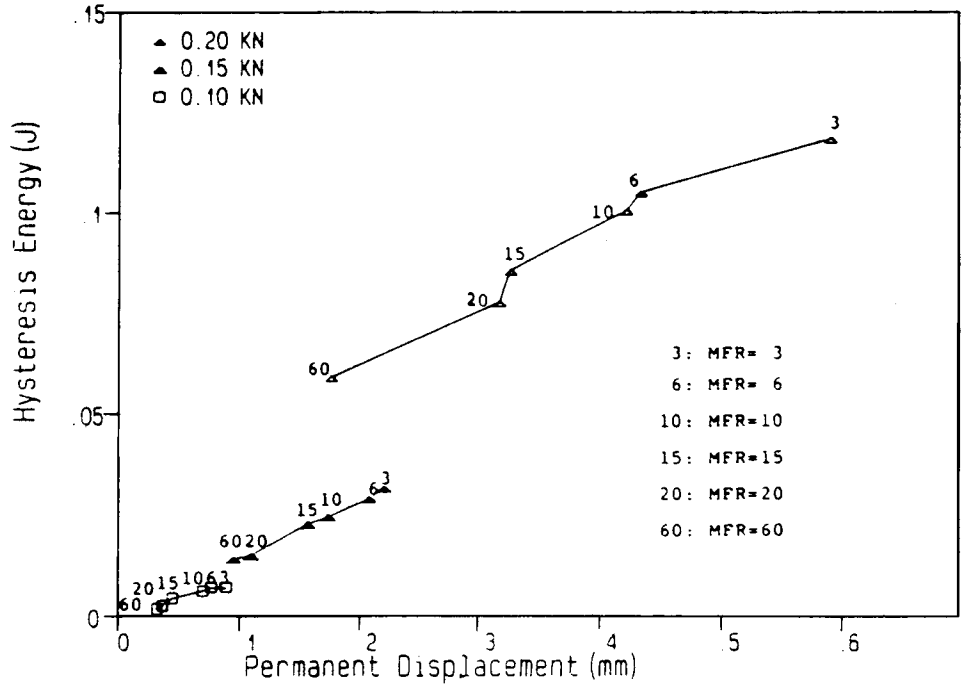

Figure 9 Relation of hysteresis energy and resultant permanent displacement for PC with various MFRs.

put energy and the corresponding percent hysteresis loss according to the following equations.

$$U_t = U_e + U_i = \int F \cdot L \tag{2}$$

$$U_i = \Phi U_t, \tag{3}$$

where the U_t, U_e, and U_i are total input energy, elastic storage energy, and inelastic loss energy, respectively. F is load and Φ is percent hysteresis loss. Assume the plastic energy, U_p, the energy consumed exclusively for plastic zone formation, has relation with the inelastic energy. The precrack plastic volume is also expected to be yield-stress-related.

$$U_p = K_1 \cdot U_i^n = K_1(\Phi \cdot U_t)^n \tag{4}$$

$$V_p = K_2 \cdot U_p / \partial_y^m = K_1 \cdot K_2 \cdot \Phi^n \cdot U_t^n / \partial_y^m, \tag{5}$$

where K_1, K_2, n, and m are constants. U_t from eq. (2) can be easily obtained from an experiment. At onset of crack initiation, $L = L_i$,

$$\text{if} \begin{cases} L_i > L_c \text{ and } V_p > V_c, & \text{ductile tearing} \\ L_i \cong L_c \text{ and } V_p \cong V_c, & \text{ductile or brittle, at transition} \\ L_i < L_c \text{ and } V_p < V_c, & \text{brittle fracture} \end{cases}$$

L_i is the crack initiation displacement. L_c and V_c are critical displacement and critical plastic volume as described above. Quantitatively, L_i is closely related to hysteresis energy as illustrated in Figures 8 and 10 and also to V_p according to eq. (5); however, its occurrence is independent of V_p. Whether L_i will exceed L_c is characteristic of the material and the experimental conditions. Therefore, L_i actually dictates V_p as the most important factor to determine whether ductile or brittle failure. Any effort to toughen the material is to delay or retard the crack initiation and allow the growth of the precrack plastic zone exceeding over the critical value (V_c). When a crack propagates through and within this precrack plastic zone, ductile tearing occurs. If the precrack plastic zone is too small at the onset of crack initiation, the momentum carried by the crack initiation can easily propagate and pass through the precrack plastic zone, and a brittle failure occurs. Figure 11 shows the diagrams of the proposed model based on precrack plastic zone to illustrate three possible types of fractures. Deformation displacement continuously increases after crack initiation, and further

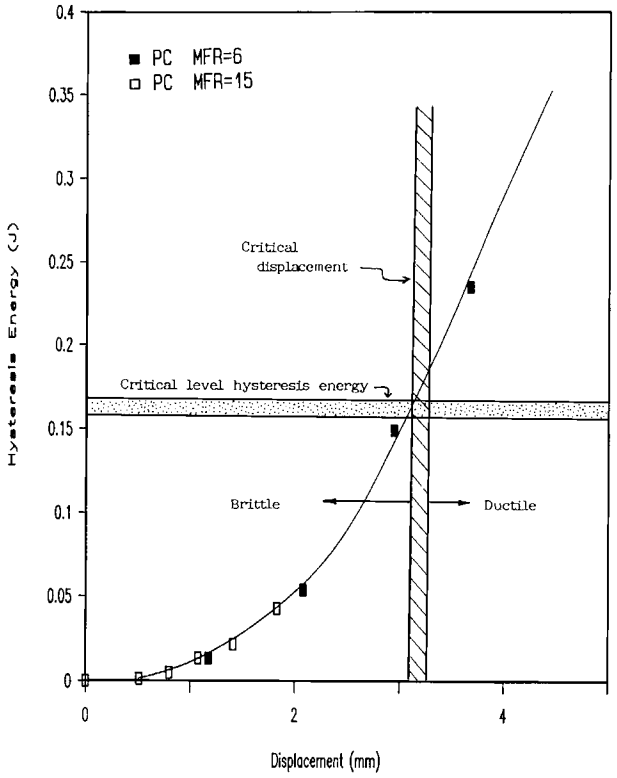

Figure 10 Determination of critical hysteresis energy for crack initiation.

extension of the plastic zone is also anticipated. The competition between the advancing cracking tip and the plastic zone forefront after onset of crack initiation can result in several unusual situations. The first unusual semiductile example is that the specimen is fracture ductile in the front portion but brittle in the back portion.[19] This so-called ductile tearing instability usually occurs on rubber-modified polyblends at high impact rates when the crack tip propagates initially within the plastic zone by ductile tearing but eventually overtakes the forefront of the plastic zone and turns into brittle fracture.[19] The second type of semiductile fracture, which has not been found and may not exist, is reverse of the first type: brittle in the front and ductile in the back. The third type of fracture occurs when the crack tip and the forefront of the plastic zone advance side by side at almost the same pace, and results in another type of semiductile fracture.[10] This third type of semiductile fracture occurs on low-temperature IZOD impact of the $\frac{1}{8}$-in. PC with large notch radius (20 mils). The recorded impact strength is about at the middle of the ductile and brittle fractures. The resultant fractured surface shows extensive localized

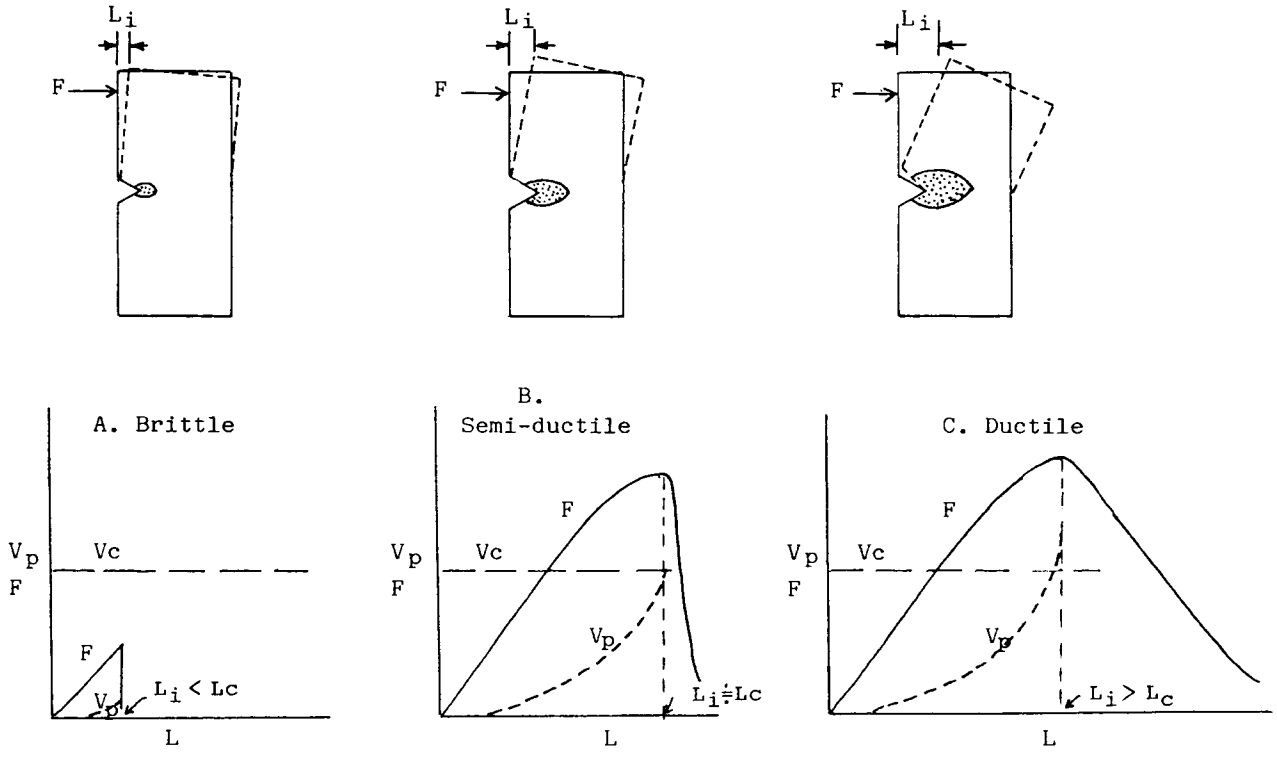

Figure 11 Diagrams illustrate three modes of fractures based of critical precrack plastic zone. A, brittle; B, semiductile; C, ductile.

shear yielding but no lateral constriction on the sides.[10] The advancing crack tip front and the dimension of the plastic zone become more complicated as the thickness of the specimen is increased from plane stress to plane strain. Yee[20] reported yet another type of semibrittle fracture for the $\frac{1}{4}$-in. PC with a flat and mirror-like triangular area that can be interpreted as a small portion of the crack tip front (most likely at middle point) runs ahead of the plastic zone forefront but most of the crack tip front is still within the plastic zone. We also observed similar results on the $\frac{1}{4}$-in. PC (MFR = 15) fractured at slow rate and high temperature.[11]

Admittedly, the above descriptions are oversimplifications of a complicated phenomenon and do not take into account the complex growing process for the crack tip front and the shape of the plastic zone. However, this proposed model based on precrack plastic zone does provide a qualitative but simple means to understand any fracture phenomenon.

CONCLUSIONS

This study intends to better understand the complicated ductile-brittle transition phenomenon and takes polycarbonates with various molecular weights as examples. The precrack hysteresis energy at the same load increases with the increase of polycarbonate molecular weight. Greater precrack hysteresis energy means less elastic storage energy available for crack initiation and greater precrack plastic zone. Precrack hysteresis energy may come from plasticity, viscoelasticity, crazes, and microvoids. By employing the pseudoductile polycarbonate matrix and with a fairly slow deformation rate, plasticity is the major contributor of the precrack hysteresis energy. Therefore, greater precrack hysteresis energy results in greater precrack plastic zone. The precrack plastic zone is increased with the increase of the deformation displacement, and such relation can be applied to different MW polycarbonates. PC MFR = 10 ($\frac{1}{4}$ inch) is at ductile-brittle transition under 10 mm/min deformation rate and the critical displacement (L_c) can be obtained. The critical hysteresis energy (and therefore the critical plastic zone volume, V_c) can be determined from the intercept of L_c and relation curve of hysteresis energy and deformation displacement. It is very clear now that the reason for the brittle failure of the lower-MW PC is due to the earlier crack initiation, and the

accumulated precrack plastic zone being too small to contain the propagating crack front, thus resulting in brittle fracture. Higher-MW PC with slightly lower yield stress and higher entanglement density is able to withstand crack initiation more effectively and allows the precrack plastic zone to grow above the critical value. Therefore, the key in toughening the precrack materials is to delay or retard the crack initiation. The addition of elastomer into polymeric matrices exactly serves such purpose and the results will be reported later. A simple model based on the critical plastic zone is proposed that is not known to conflict with any models currently existing.

The authors are grateful to the National Science Council of Republic of China for the financial support and Polycarbonate Research Department of Dow Chemical Company for the polycarbonate samples.

REFERENCES

1. G. L. Pitman, I. M. Ward, and R. A. Duckett, *J. Mater. Sci.*, **13,** 2092 (1978).
2. A. J. Kinloch and R. J. Young, *Fracture Behavior of Polymers,* Elsevier Applied Science Publishers, London, 1985, pp. 237–239.
3. J. H. Golden, B. L. Hammant, and E. A. Hazell, *J. Polym. Sci.*, **A2,** 4787 (1964).
4. B. H. Bersted, *J. Appl. Polym. Sci.*, **24,** 37 (1979).
5. D. G. Legrand, *J. Appl. Polym. Sci.*, **13,** 2129 (1969).
6. J. T. Ryan, *Polym. Eng. Sci.*, **18,** 267 (1978).
7. F. C. Chang and L. H. Chu, *J. Appl. Polym. Sci.*, to appear.
8. F. C. Chang and L. H. Chu, Proc. IUPAC, Korea, 8-1-21 (1989).
9. G. L. Pitman and I. M. Ward, *Polymer,* **22,** 1745 (1981).
10. F. C. Chang and L. H. Chu, *Polym. Mater.: Sci. Eng.*, **60,** 851 (1989).
11. H. C. Hsu and F. C. Chang, *Proc. Annual Conf. of Chinese Soc. for Mater. Sci.*, Taiwan, 1990, p. 1005.
12. H. C. Hsu and F. C. Chang, *Proc. 13th ROC Polym. Symp.*, Taiwan, 1990, p. 796.
13. F. C. Chang and H. C. Hsu, *Polym. Mater.: Sci. Eng.*, **62,** 106 (1990).
14. F. C. Chang and H. C. Hsu, *China-Japan Bilateral Symp. on Polym. Sci. Mater.*, China, 1990.
15. F. C. Chang and M. Y. Yang, *Polym. Eng. Sci.*, **30,** 543 (1990).
16. F. C. Chang, unpublished data.
17. I. Narisawa and M. T. Takemori, *Polym. Eng. Sci.*, **28,** 1462 (1988).
18. I. Narisawa and M. T. Takemori, *Polym. Eng. Sci.*, **29,** 671 (1989).
19. M. E. J. Dekkers and S. Y. Hobbs, *Polym. Eng. Sci.*, **27,** 1164 (1987).
20. A. F. Yee, *J. Mater. Sci.*, **12,** 757 (1977).

Received August 15, 1990
Accepted December 7, 1990